

# Stability of quark matter affected by the surface tension in a strong magnetic field

Yu-Ying He and Xin-Jian Wen

*Institute of Theoretical Physics, State Key Laboratory of Quantum Optics and Quantum Optics Devices,  
Shanxi University, Taiyuan, Shanxi 030006, China*

The surface tension of quark matter in a strong magnetic field is investigated using a geometric approach. The interface between the hadronic phase and quark phase is determined by the Maxwell construction of the first-order transition. When surface tension is included, the free energy per baryon is no longer a monotonic function of the chemical potential. Specifically, for smaller droplets, a larger chemical potential is required to achieve a stable phase. Moreover, we find that the surface tension does not increase monotonically with the magnetic field. Finally, it is shown that stable quark matter, both with and without surface tension, can exist at a specific magnetic field strength, which would provide favorable conditions for the experimental production of quark matter.

## I. INTRODUCTION

Up to now, it is well known that strong magnetic fields are relevant in the early universe, magnetars, and non-central heavy ion collisions. They produce significant effects on the equation of state in compact stars and the QCD phase diagram. In particular, magnetic catalysis and inverse magnetic catalysis in the QCD chiral transition have been confirmed by lattice calculations [1, 2]. The magnetic catalysis effect shows that a magnetic field enhances the spontaneous breakdown of chiral symmetry [3–9]. A more general result states that a constant magnetic field leads to the generation of a fermion dynamical mass [10]. This surprising and unexpected inverse catalysis at finite temperatures was first predicted in lattice simulations [11, 12]. The corresponding theoretical interpretation is supported by investigations of the running coupling constant and/or the anomalous magnetic moment. In all of these processes, the magnetic effect is demonstrated through changes in the order parameter of chiral symmetry. The inclusion of baryon density drastically changes the situation, and the transition becomes first-order. At high densities, the matter is always in the chirally symmetric phase. Furthermore, the formation of bubbles can be understood as a natural consequence of the first-order nature of the phase transition. The transition from the chiral symmetry broken hadron phase to the chiral symmetry restored quark phase is a first-order phase transition. The bubble formation of a quark phase in hadronic matter can be studied through a nucleation process. These bubbles may consist of matter with restored chiral symmetry, while the surrounding hadronic matter remains in the chiral symmetry broken phase. Therefore, the study of bubbles composed of mixed phases is of great interest in the presence of a strong magnetic field.

Although the study of QCD phase transitions has made significant progress, the realistic occurrence of such transitions could be influenced by the finite volume of the system. Most model descriptions of strong interactions at high density and low temperature suggest a first-order phase transition for both the chiral and deconfinement transitions. Therefore, the interface composed of the two phases plays an important role. The surface tension [13–24] is defined as the excess free energy of a two-phase configuration containing a bubble wall, compared to a homogeneous, one-phase configuration, per unit wall surface area [25]. The investigation of surface tension and its impact on the stability of quark matter has been widely studied in the MIT bag model and the density-dependent quark mass model. However, their descriptions of interface tension lack detailed information about the phase transition. The quark quasiparticle model, as an extension of the bag model, has been developed to study the bulk properties of dense quark matter at finite density and temperature [2, 26–28]. This model provides a framework for understanding the medium effect on surface tension [29]. To describe the chiral phase transition and dynamical symmetry breaking, the Nambu-Jona-Lasinio (NJL) model is widely used in QCD-like investigations [30–32]. It effectively explains the surface tension at finite temperature, which is constructed by the mixed phase in the context of chiral symmetry breaking [33].

The surface tension is a characteristic property of coexisting phases. For example, the magnitude of the surface tension between a liquid drop and a gas phase plays a dominant role in the formation of raindrops. For QCD matter, the surface tension is a fundamental parameter for understanding finite-size effects and nucleation phase transitions [34]. However, the surface tension between the true vacuum and the perturbative phase is often neglected in comparison to the confinement bag constant. For the mixed phase to occur, the surface tension at the interface separating the quark and hadron phases should be relatively small [35, 36]. A large value of the surface tension, such as  $29.73 \text{ MeV}\cdot\text{fm}^{-2}$ , may be insufficient to stabilize quark matter during the phase transition. It has been proposed that strange matter could not have survived in the early Universe because it might boil and form bubbles of hadronic gas [37]. The study of surface tension should be considered a complementary approach to understanding QCD at finite density, as lattice QCD (LQCD) methods are insufficient to determine the structure of matter at larger chemical potentials. The aim of this work is to investigate the surface tension of cold quark matter in the NJL model under strong magnetic fields. We hope to explore the stability of quark matter modified by surface tension in a finite volume.

This paper is organized as follows. In Section II, we present the thermodynamics of the magnetized quark matter in the NJL model. The geometric approach is employed to define the surface tension in Section III. The numerical results on the stability of quark matter are presented in Section IV. The last section provides a brief summary.

## II. THERMODYNAMICS OF NJL MODEL IN A STRONG MAGNETIC FIELD

The starting point of the NJL model as an effective theory is the Lagrangian density, which models dynamical chiral symmetry breaking. The Lagrangian density of the two-flavor NJL model in a strong magnetic field is given by [38, 39]:

$$\mathcal{L}_{NJL} = \bar{\psi}(iD - m)\psi + G[(\bar{\psi}\psi)^2 + (\bar{\psi}i\gamma_5\vec{\tau}\psi)^2] - \frac{1}{4}F_{\mu\nu}F^{\mu\nu}, \quad (1)$$

where  $\psi$  represents a flavor isodoublet (u and d quarks), and  $\vec{\tau}$  are isospin Pauli matrices. The covariant derivative  $D_\mu = \partial_\mu - iQeA_\mu$  represents the coupling of the quarks to the electromagnetic field, and a sum over flavor and color degrees of freedom is implicit. Here,  $Q = \text{diag}(q_u, q_d) = \text{diag}(2/3, -1/3)$  is the quark electric charge matrix in flavor space. The Abelian gauge field  $A_\mu$  stands for the external magnetic field  $B$  aligned along the z-direction. In the mean-field approximation[40, 41], the dynamical quark mass is directly dependent on the quark condensate[42]:

$$M_i = m - 2G\langle\bar{\psi}\psi\rangle, \quad (2)$$

where the current masses  $m_u = m_d = m$  are used, and the quark condensates include contributions from u and d quarks as  $\langle\bar{\psi}\psi\rangle = \sum_{i=u,d}\phi_i$ . For the SU(2) version, although the quark condensates for the flavors u and d in the presence of a magnetic field are different due to their different electric charges, the masses of the  $u$  and  $d$  constituent quarks are equal to each other in the isospin symmetric limit. The constituent mass depends on both condensates, and thus the same mass  $M_u = M_d = M$  is obtained for u and d quarks. The contribution from the quark flavor  $i$  is given by [43]:

$$\phi_i = \phi_i^{\text{vac}} + \phi_i^{\text{mag}} + \phi_i^{\text{med}}. \quad (3)$$

The terms  $\phi_i^{\text{vac}}$ ,  $\phi_i^{\text{mag}}$ , and  $\phi_i^{\text{med}}$  represent the vacuum, magnetic field, and medium contributions to the quark condensation, respectively,[44, 45]

$$\begin{aligned} \phi_i^{\text{vac}} &= -\frac{MN_c}{2\pi^2} \left[ \Lambda\sqrt{\Lambda^2 + M^2} - M^2 \ln\left(\frac{\Lambda + \sqrt{\Lambda^2 + M^2}}{M}\right) \right], \\ \phi_i^{\text{mag}} &= -\frac{M|q_i|BN_c}{2\pi^2} \left\{ \ln[\Gamma(x_i)] - \frac{1}{2}\ln(2\pi) + x_i - \frac{1}{2}(2x_i - 1)\ln(x_i) \right\}, \\ \phi_i^{\text{med}} &= \sum_{k_i=0} a_{k_i} \frac{M|q_i|BN_c}{2\pi^2} \ln\left(\frac{\mu + \sqrt{\mu^2 - M_n^2}}{M_n}\right), \end{aligned} \quad (4)$$

where  $a_{k_i} = 2 - \delta_{k_0}$  and  $k_i$  are the degeneracy label and the Landau quantum number, respectively. The dimensionless quantity  $x_i$  is defined as  $x_i = M^2/(2|q_i|B)$ .  $M_n = \sqrt{M^2 + 2k_i|q_i|B}$ .

The total thermodynamic potential density in the mean-field approximation is:

$$\Omega = \frac{(M - m_0)^2}{4G} + \sum_{i=u,d} \Omega_i, \quad (6)$$

where the first term is the interaction term. In the framework of the magnetic-field-independent regularization [46–48], the thermodynamic potential  $\Omega_i$  is usually divided into three terms:

$$\Omega_i = \Omega_i^{\text{vac}} + \Omega_i^{\text{mag}} + \Omega_i^{\text{med}}. \quad (7)$$

The vacuum contribution to the thermodynamic potential is

$$\Omega_i^{\text{vac}} = \frac{N_c}{8\pi^2} \left[ M^4 \ln\left(\frac{\Lambda + \epsilon_\Lambda}{M}\right) - \epsilon_\Lambda \Lambda(\Lambda^2 + \epsilon_\Lambda^2) \right], \quad (8)$$

where  $\epsilon_\Lambda = \sqrt{\Lambda^2 + M^2}$ . The ultraviolet divergence in the vacuum part  $\Omega_i^{\text{vac}}$  of the thermodynamic potential is removed by the momentum cutoff. The magnetic field and medium contributions are respectively [44, 45, 49]:

$$\Omega_i^{\text{mag}} = -\frac{N_c(|q_i|B)^2}{2\pi^2} \left[ \zeta'(-1, x_i) - \frac{1}{2}(x_i^2 - x_i) \ln(x_i) + \frac{x_i^2}{4} \right], \quad (9)$$

$$\Omega_i^{\text{med}} = -\sum_{k_i=0} a_{k_i} \frac{|q_i|BN_c}{4\pi^2} \left\{ \mu \sqrt{\mu^2 - M_n^2} - M_n^2 \ln \left( \frac{\mu + \sqrt{\mu^2 - M_n^2}}{M_n} \right) \right\}, \quad (10)$$

where  $\zeta(a, x) = \sum_{n=0}^{\infty} \frac{1}{(a+n)^x}$  is the Hurwitz zeta function [43].

### III. THE SURFACE TENSION IN A GEOMETRIC APPROACH

In literature, surface tension has been investigated using two main approaches. One is the multiple reflection expansion approximation [50], and the other is the geometric approach [33, 51]. The latter method incorporates more information about the interaction. In this section, we review the geometric approach for calculating surface tension, which was first proposed in Ref. [52, 53]. For any subcritical temperature  $T < T_c$ , two phases with different densities can reach thermodynamic equilibrium in phase coexistence. When these two phases come into contact, a mechanically stable interface forms between them, and the surface tension  $\gamma_T$  characterizes this interface. As the temperature gradually increases from 0 to  $T_c$ , the two densities coincide at the critical temperature  $T_c$ , and the surface tension eventually vanishes.

The free energy density  $f_T(\rho)$  can be expressed as:  $f_T(\rho) = \mathcal{E}_T(\rho) - T s_T(\rho) = \mu_T(\rho)\rho - P_T(\rho)$ , which includes the fundamental relation of the energy density  $\mathcal{E}_T$  and the pressure  $P_T$ . When  $f_T(\rho)$  exhibits local concavity, it indicates that the system in that region is unstable. As a result, the system will tend to decompose into two phases: a low-density phase  $\rho_1(T)$  and a high-density phase  $\rho_2(T)$ . To achieve thermodynamic equilibrium between these two phases, a common tangent of the free energy at densities  $\rho_1$  and  $\rho_2$  corresponds to a common chemical potential and defines the Maxwell free energy density  $f_T^M(\rho)$ . Consequently, the cost of the free energy density, defined as  $\Delta f_T(\rho) \equiv f_T(\rho) - f_T^M(\rho) \geq 0$ , is non-negative.

The interface tension  $\gamma_T$  is given by

$$\gamma_T = a \int_{\rho_1}^{\rho_2} \frac{d\rho}{\rho g} [2\mathcal{E}_g \Delta f_T(\rho)]^{\frac{1}{2}}, \quad (11)$$

where  $\rho_g$  is a characteristic value of the density,  $\mathcal{E}_g$  is a characteristic value of the energy density, and the parameter  $a \approx 1/m_\sigma \approx 0.33$  fm.

In the zero-temperature limit, the interface tension is controlled by the magnetic field. The free energy density is given by the following equation:

$$f = \mu\rho - P = \mu\rho + \Omega, \quad (12)$$

$$\Delta f = (\Omega - \Omega_M) + \rho(\mu - \mu_M), \quad (13)$$

where  $P$  is the pressure,  $\Omega$  is the thermodynamic potential density,  $\mu$  is the quark chemical potential, and  $\rho$  is the quark number density. Here,  $\Omega_M$  and  $\mu_M$  are the thermodynamic potential density and quark chemical potential of the Maxwell structure, respectively. A more detailed discussion can be found in Ref. [33, 54]

For the case of a finite spherical droplet, we assume spherical symmetry with radius  $R$ . The total free energy is expressed as a sum of the volume and surface terms:

$$f = (\mu\rho + \Omega)V + \gamma S, \quad (14)$$

where  $V$  is the volume and  $S$  is the surface area. Correspondingly, the free energy per baryon, including the coexisting phases, is given by

$$\frac{f}{A} = \frac{\Omega}{\rho_B} + 3\mu + \frac{3\gamma}{\rho_B R}, \quad (15)$$

where  $A$  is the baryon number, and the baryonic density  $\rho_B$  can be written as [43]

$$\rho_B = \frac{1}{3}(\rho_u + \rho_d) = \sum_{i=u}^d \sum_{k_i=0}^{k_i^{\text{max}}} a_{k_i} \frac{|q_i|BN_c}{6\pi^2} \sqrt{\mu^2 - 2k_i|q_i|B - M^2}. \quad (16)$$

#### IV. NUMERICAL RESULT AND CONCLUSION

In this section, we present numerical results for the surface tension between the chiral broken phase and the chiral restored phase. Furthermore, we demonstrate that the stability of finite-size quark matter is influenced by the surface tension. In our model, the following parameters are adopted for the evaluation:  $m_u = m_d = 5.6$  MeV,  $\Lambda = 631$  MeV,  $G = 2.19/\Lambda^2$ .

By solving the gap equation (2), the obtained effective mass is used to determine the thermodynamic potential density. The free energy density  $f$  can then be calculated to determine the difference  $\Delta f$ , which is a crucial ingredient in the evaluation of surface tension. For more detailed references, see Refs. [33, 54]. In Fig. 1, the variation of constituent quark mass  $M$  is shown as a function of quark chemical potential  $\mu$  at  $T \rightarrow 0$  for  $eB = 0.2$  GeV<sup>2</sup>. The black solid line represents the stable solutions of the dynamical mass  $M$ , while the red dashed line represents the unstable solutions in the first-order transition. The Maxwell line is determined by the black dashed line. The dynamical quark mass remains constant in the vacuum and becomes multivalued as the chemical potential increases up to  $\mu \sim 280$  MeV, which marks the beginning of a first-order transition. The purely chiral symmetry restored phase emerges when the chemical potential exceeds  $\mu = 374$  MeV. Thus, the quark chemical potential range of 280 MeV to 374 MeV corresponds to the coexisting phases at the magnetic field  $eB = 0.2$  GeV<sup>2</sup>. There exists a kink for the dynamical quark mass at around  $\mu = 370$  MeV. This is produced by the Landau level quantization effect. The strong magnetic field causes the discretization of quark energy levels. When the Fermi surface crosses a Landau level, it leads to a sudden change in the density of states and the effective mass.

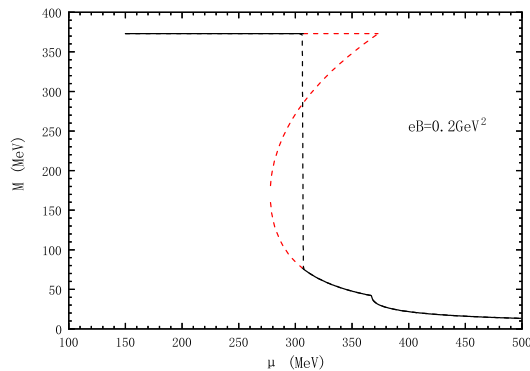


FIG. 1: The variation of the constituent quark mass  $M$  with the quark chemical potential  $\mu$  is shown. The red dashed line and the black solid line represent the unstable and stable solutions, respectively. The black dashed line represents the Maxwell construction.

In our study, a spherical system composed of the chiral broken and restored phases is assumed to investigate the finite-size effect. The electric field configurations determine the droplet size and the geometry of structures [55]. When discussing relatively short-distance effects, one may disregard spatial changes in sphericity due to the presence of a strong magnetic field. The free energy of the system can be expressed as the sum of the bulk matter term and the surface term. The free energy per baryon  $f/A$  is shown as a function of the density  $\rho$  for a given radius  $R = 10$  fm in Fig. 2. It is evident that, when surface tension is considered, the free energy per baryon initially decreases and then increases as the density increases, as shown in the inset of Fig 2, where the solid dot indicates the position of the minimum. Without surface tension, the free energy per baryon, marked by the red line, remains a monotonically increasing function of density. Moreover, the inclusion of surface tension always results in a higher free energy per baryon compared to that of bulk matter. Consequently, it is concluded that surface tension reduces the thermodynamic stability of quark matter.

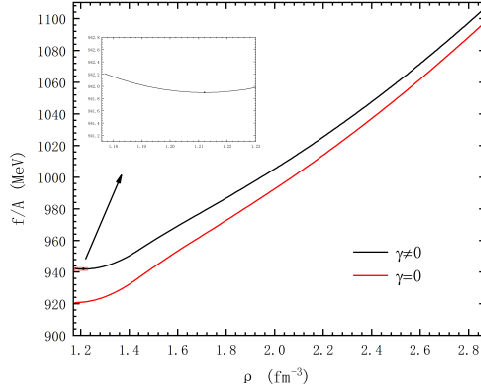


FIG. 2: The free energy per baryon  $f/A$  as a function of the quark number density  $\rho$  is shown, both with and without surface tension, at  $eB = 0.2 \text{ GeV}^2$ .

Spherical radii of  $R = 5, 10, 30 \text{ fm}$  are adopted for comparison. In Fig. 3, the free energy per baryon  $f/A$  is shown as a function of quark chemical potential. When the surface tension is taken into account, the non-monotonic behavior becomes clearly evident and is more pronounced than that in Fig. 2. The free energy per baryon initially decreases and then increases as the chemical potential increases. The minimum values of  $f/A$ , marked by solid dots in red, blue, and green, are reached at the following points:  $R = 5 \text{ fm}$  and  $\mu = 321 \text{ MeV}$  (red dot),  $R = 10 \text{ fm}$  and  $\mu = 314 \text{ MeV}$  (blue dot), and  $R = 30 \text{ fm}$  and  $\mu = 309 \text{ MeV}$  (green dot). As the radius increases, the position of the minimum free energy per baryon shifts toward lower chemical potentials. For sufficiently large radii, the behavior approaches the monotonic curve of bulk matter, indicated by the black line at the bottom. For smaller radii, a larger chemical potential is required to stabilize the spherical volume. In general, it is confirmed that surface tension significantly increases the free energy per baryon due to the interface contribution.

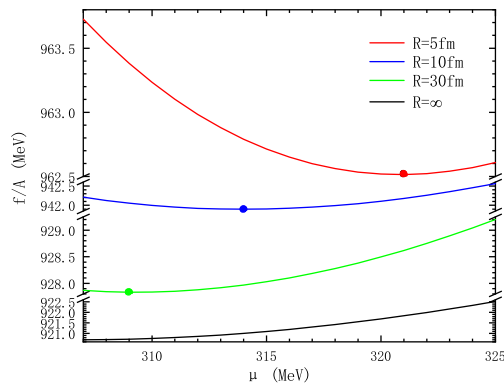


FIG. 3: The free energy per baryon  $f/A$  as a function of the quark chemical potential  $\mu$  is shown for  $\gamma \neq 0$  (at  $eB = 0.2 \text{ GeV}^2$ ) and radii  $R=5, 10, \text{ and } 30 \text{ fm}$ . The monotonic line at the bottom corresponds to the bulk matter case ( $R = \infty$ ).

Fig. 4 illustrates the free energy per baryon as a function of the finite droplet radius  $R$  at fixed magnetic fields of  $eB = 0.1, 0.2, \text{ and } 0.3 \text{ GeV}^2$ . The horizontal dashed lines represent the corresponding values for bulk quark matter. As the radius increases, the free energy per baryon gradually decreases and eventually approaches the constant value of bulk matter. It is evident that surface tension has a more significant effect on the increase of the free energy per baryon at small droplet sizes. Consequently, the stability of the quark matter system is reduced by the surface energy. By comparing the results for different magnetic fields, it is found that the effect of surface tension is more pronounced for stronger magnetic fields. For the magnetic field  $eB = 0.3 \text{ GeV}^2$ , the free energy per baryon increases by approximately 3 percent compared to that of bulk matter.

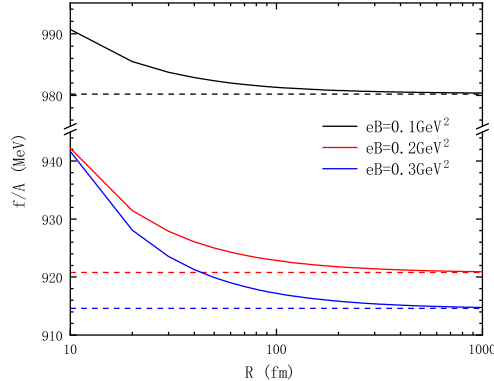


FIG. 4: The free energy per baryon as a function of the radius of a finite droplet is shown for  $eB = 0.1, 0.2,$  and  $0.3 \text{ GeV}^2$ , with the radius  $R$  varying from 10 fm to 1000 fm.

To explore the effects of the magnetic field and surface tension on the stability of quark matter, we investigate the variation of the free energy with respect to the magnetic field. Fig. 5 presents the free energy per baryon as a function of the magnetic field on the left axis. The free energy with and without surface tension is marked by the black and the red lines, respectively. These two lines both reach their minimum values at a magnetic field strength of  $0.26 \text{ GeV}^2$ , after which they begin to rise steadily, indicating the existence of a stable phase at an appropriate magnetic field strength. The difference between these two lines increases with the magnetic field strength in the range of  $0.04 \text{ GeV}^2$  to  $0.26 \text{ GeV}^2$ . When the magnetic field strength exceeds  $0.26 \text{ GeV}^2$ , the difference between the two lines gradually approaches a constant. In the magnetic field range of  $0.04 \text{ GeV}^2$  to  $0.06 \text{ GeV}^2$ , the near overlap of the two lines is due to the very small surface tension at these magnetic fields, as indicated by the black arrow in the figure.

The surface tension is shown on the right axis in Fig. 5. It exhibits a non-monotonic dependence on the magnetic field, reaching its minimum value at  $0.06 \text{ GeV}^2$ . The blue dots illustrate the variation of surface tension with magnetic field as reported in Ref. [[33]]. Compared to our results, which are represented by the black dotted line, the small discrepancy is led to by the parameter set in the model. Furthermore, the trends observed in the two datasets demonstrate a notable alignment to some extent.

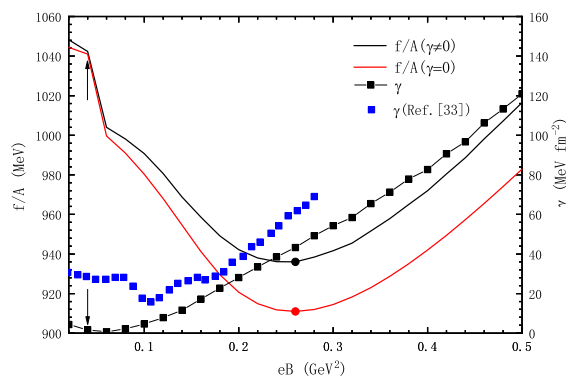


FIG. 5: The free energy per baryon on the left axis and the surface tension on the right axis are shown as functions of the magnetic field. The blue points correspond to the variation of surface tension with the magnetic field, as reported in Ref. [[33]].

## V. SUMMARY

In this work, we have investigated the surface tension related to the first-order chiral phase transition of two-flavor magnetized quark matter within the NJL model. The surface tension is defined through a geometric approach. The Maxwell construction is required to determine the equation of state in the coexisting phase. By assuming a spherical

volume for the system, we have analyzed the variation of the free energy per baryon with respect to quark number density and quark chemical potential. It has been shown that the free energy per baryon depends on the finite droplet radius and magnetic field strength. Our results indicate that the free energy per baryon, when including surface tension, is not a monotonic function of increasing baryon density and quark chemical potential. The stable chemical potential is determined by the minimum free energy per baryon, which depends on the droplet radius. Specifically, smaller droplets in the coexisting phase require a larger chemical potential. Moreover, the free energy per baryon with surface tension is always higher than that of bulk matter. This suggests that the inclusion of surface tension inevitably reduces the stability of quark matter. It is also shown that the free energy per baryon decreases as the spherical radius increases, eventually approaching the bulk limit.

The surface tension coefficient is a significantly increasing function of the magnetic field for  $0.06 \text{ GeV}^2 < eB < 0.26 \text{ GeV}^2$ . However, at  $eB = 0.06 \text{ GeV}^2$ , the surface tension is minimal, and consequently, the finite size has a weak influence on the free energy. Finally, it has been demonstrated that stable quark matter exists at an appropriate magnetic field, regardless of whether surface tension is included. We argue that such a proper magnetic field condition is favorable for producing the quark-gluon phase in experiments.

### Acknowledgments

The authors would like to thank support from the National Natural Science Foundation of China under the Grant Nos. 11875181 and 12047571. This work was also sponsored by the Fund for Shanxi "1331 Project" Key Subjects Construction.

- 
- [1] R. D. Pisarski, *Physica A* **158**, 146-157 (1989)
  - [2] K. Schertler, C. Greiner and M. H. Thoma, *Nucl. Phys. A* **616**, 659-679 (1997) doi:10.1016/S0375-9474(97)00014-6 [arXiv:hep-ph/9611305 [hep-ph]].
  - [3] S. P. Klevansky and R. H. Lemmer, *Phys. Rev. D* **39**, 3478 (1989) doi:10.1103/PhysRevD.39.3478.
  - [4] V. P. Gusynin, V. A. Miransky, and I. A. Shovkovy, *Phys. Lett. B* **349**, 477 (1995) doi:10.1016/0370-2693(95)00232-A [arXiv: hep-ph/9412257 [hep-ph]].
  - [5] I. A. Shushpanov and A. V. Smilga, *Phys. Lett. B* **402**, 351 (1997) doi:10.1016/S0370-2693(97)00441-3 [arXiv:hep-ph/9703201 [hep-ph]].
  - [6] E. J. Ferrer and V. de la Incera, *Phys. Lett. B* **481**, 287 (2000) doi:10.1016/S0370-2693(00)00482-2 [arXiv:hep-ph/0004113 [hep-ph]].
  - [7] N. Mueller and J. M. Pawłowski, *Phys. Rev. D* **91**, 116010 (2015) doi:10.1103/PhysRevD.91.116010 [arXiv:1502.08011 [hep-ph]].
  - [8] V. A. Miransky and I. A. Shovkovy, *Phys. Rev. D* **66**, 045006 (2002) doi:10.1103/PhysRevD.66.045006 [arXiv:hep-ph/0205348 [hep-ph]].
  - [9] T. Inagaki, D. Kimura, and T. Murata, *Prog. Theor. Phys.* **111**, 371 (2004) doi:10.1143/PTP.111.371 [arXiv:hep-ph/0312005 [hep-ph]].
  - [10] V. P. Gusynin, V. A. Miransky and I. A. Shovkovy, *Phys. Rev. Lett.* **73**, 3499-3502 (1994) doi:10.1103/PhysRevLett.73.3499 [arXiv:hep-ph/9405262 [hep-ph]].
  - [11] F. Preis, A. Rebhan and A. Schmitt, *JHEP* **03**, 033 (2011) doi:10.1007/JHEP03(2011)033 [arXiv:1012.4785 [hep-th]].
  - [12] G. S. Bali, F. Bruckmann, G. Endrodi, Z. Fodor, S. D. Katz, S. Krieg, A. Schafer and K. K. Szabo, *JHEP* **02**, 044 (2012) doi:10.1007/JHEP02(2012)044 [arXiv:1111.4956 [hep-lat]].
  - [13] M. Oertel and M. Urban, *Phys. Rev. D* **77**, 074015 (2008) doi:10.1103/PhysRevD.77.074015 [arXiv: 0801.2313 [nucl-th]].
  - [14] B. W. Mintz, R. Stiele, R. O. Ramos, and J. Schaffner-Bielich, *Phys. Rev. D* **87**, 036004 (2013) doi:10.1103/PhysRevD.87.036004 [arXiv: 1212.1184 [hep-ph]].
  - [15] Ke, Wei-yao and Liu, Yu-xin, *Phys. Rev. D* **89**, 074041 (2014) doi:10.1103/PhysRevD.89.074041 [arXiv: 1312.2295 [hep-ph]].
  - [16] F. Gao and Y. Liu, *Phys. Rev. D* **94**, 094030 (2016) doi:10.1103/PhysRevD.94.094030 [arXiv: 1609.08038 [hep-ph]].
  - [17] C. J. Xia, G. X. Peng, T. T. Sun, W. L. Guo, D. H. Lu, and P. Jaikumar, *Phys. Rev. D* **98**, 034031 (2018) doi:10.1103/PhysRevD.98.034031 [arXiv: 1808.07655 [hep-ph]].
  - [18] E. S. Fraga, M. Hippert, and A. Schmitt, *Phys. Rev. D* **99**, 014046 (2019) doi:10.1103/PhysRevD.99.014046 [arXiv: 1810.13226 [hep-ph]].
  - [19] G. Lugones and A. G. Grunfeld, *Phys. Rev. C* **99**, 035804 (2019) doi:10.1103/PhysRevC.99.035804 [arXiv: 1811.09954 [astro-ph.HE]].
  - [20] R. S. Bogadi, M. Govender, and S. Moyo, *Phys. Rev. D* **102**, 043026 (2020) doi:10.1103/PhysRevD.102.043026.
  - [21] G. Lugones and A. G. Grunfeld, *Phys. Rev. C* **103**, 035813 (2021) doi:10.1103/PhysRevC.103.035813 [arXiv: 2010.06098 [nucl-th]].

- [22] D. N. Voskresensky, *Prog. Part. Nucl. Phys.* **130**, 104030 (2023) doi:10.1016/j.pnpnp.2023.104030 [arXiv: 2207.03212 [nucl-th]].
- [23] M. Mariani and G. Lugones, *Phys. Rev. D* **109**, 063022 (2024) doi:10.1103/PhysRevD.109.063022 [arXiv: 2308.13973 [nucl-th]].
- [24] C. J. Xia, T. Maruyama, N. Yasutake, and T. Tatsumi, *Phys. Rev. D* **110**, 114024 (2024) doi:10.1103/PhysRevD.110.114024 [arXiv: 2409.12489 [nucl-th]].
- [25] G. Endrődi, T. G. Kovács and G. Markó, *Phys. Rev. Lett.* **127**, no.23, 232002 (2021) doi:10.1103/PhysRevLett.127.232002 [arXiv:2109.03668 [hep-lat]].
- [26] M. Bluhm, Ph.D. thesis (2008)
- [27] M. A. Thaler, R. A. Schneider and W. Weise, *Phys. Rev. C* **69**, 035210 (2004) doi:10.1103/PhysRevC.69.035210 [arXiv:hep-ph/0310251 [hep-ph]].
- [28] Y. Y. He and X. J. Wen, *Phys. Rev. D* **107**, 074030 (2023) doi:10.1103/PhysRevD.107.074030 [arXiv:2304.03491 [hep-ph]].
- [29] X. J. Wen, J. Y. Li, J. Q. Liang and G. X. Peng, *Phys. Rev. C* **82**, 025809 (2010) doi:10.1103/PhysRevC.82.025809
- [30] E. J. Ferrer, V. delalncera, I. Portillo, and M. Quiroz, *Phys. Rev. D* **89**, 085034 (2014) doi:10.1103/PhysRevD.89.085034 [arXiv:1311.3400 [nucl-th]].
- [31] S. S. Avancini, R. L. S. Farias, N. N. Scoccola, and W. R. Tavares, *Phys. Rev. D* **99**, 116002 (2019) doi:10.1103/PhysRevD.99.116002 [arXiv:1904.02730 [hep-ph]].
- [32] P. Allen, A. G. Grunfeld, and N. N. Scoccola, *Phys. Rev. D* **92**, 074041 (2015) doi:10.1103/PhysRevD.92.074041 [arXiv:1508.04724 [hep-ph]].
- [33] A. F. Garcia and M. B. Pinto, *Phys. Rev. C* **88**, no.2, 025207 (2013) doi:10.1103/PhysRevC.88.025207 [arXiv:1306.3090 [hep-ph]].
- [34] S. Huang, J. Potvin, C. Rebbi, and S. Sanielevici, *Phys. Rev. D* **42**, 2864 (1990) doi:10.1103/PhysRevD.42.2864.
- [35] T. Maruyama, S. Chiba, H. J. Schulze and T. Tatsumi, *Phys. Rev. D* **76**, 123015 (2007) doi:10.1103/PhysRevD.76.123015 [arXiv:0708.3277 [nucl-th]].
- [36] M. G. Alford, K. Rajagopal, S. Reddy and F. Wilczek, *Phys. Rev. D* **64**, 074017 (2001) doi:10.1103/PhysRevD.64.074017 [arXiv:hep-ph/0105009 [hep-ph]].
- [37] C. Alcock and A. Olinto, *Phys. Rev. D* **39**, 1233 (1989) doi:10.1103/PhysRevD.39.1233
- [38] Y. Nambu and G. Jona-Lasinio, *Phys. Rev.* **122**, 345 (1961) doi:10.1103/PhysRev.122.345.
- [39] Y. Nambu and G. Jona-Lasinio, *Phys. Rev.* **124**, 246 (1961) doi:10.1103/PhysRev.124.246.
- [40] C. Ratti, *Europhys. Lett.* **61**, 314 (2003) doi:10.1209/epl/i2003-00171-0 [arXiv: hep-ph/0210295 [hep-ph]].
- [41] M. Buballa and M. Oertel, *Phys. Lett. B* **457**, 261-267 (1999) doi:10.1016/S0370-2693(99)00533-X [arXiv:hep-ph/9810529 [hep-ph]].
- [42] M. Buballa, *Phys. Rep.* **407**, 205 (2005) doi:10.1016/j.physrep.2004.11.004 [arXiv: hep-ph/0402234 [hep-ph]].
- [43] D. P. Menezes, M. B. Pinto, S. S. Avancini, A. P. Martinez and C. Providencia, *Phys. Rev. C* **79**, 035807 (2009) doi:10.1103/PhysRevC.79.035807 [arXiv:0811.3361 [nucl-th]].
- [44] D. P. Menezes, M. Benghi Pinto, S. S. Avancini and C. Providência, *Phys. Rev. C* **80**, 065805 (2009) doi:10.1103/PhysRevC.80.065805 [arXiv:0907.2607 [nucl-th]].
- [45] S. S. Avancini, D. P. Menezes and C. Providência, *Phys. Rev. C* **83**, 065805 (2011) doi:10.1103/PhysRevC.83.065805.
- [46] D. Ebert, K. G. Klimenko, M. A. Vdovichenko, and A. S. Vshivtsev, *Phys. Rev. D* **61**, 025005 (1999) doi:10.1103/PhysRevD.61.025005 [arXiv: hep-ph/9905253 [hep-ph]].
- [47] M. A. Vdovichenko, A. S. Vshivtsev, and K. G. Klimenko, *Phys. At. Nucl.* **63**, 470 (2000) doi:10.1134/1.855661.
- [48] I. E. Frolov, V. C. Zhukovsky, and K. G. Klimenko, *Phys. Rev. D* **82**, 076002 (2010) doi:10.1103/PhysRevD.82.076002 [arXiv: 1007.2984 [hep-ph]].
- [49] D. P. Menezes, M. B. Pinto and C. Providência, *Phys. Rev. C* **91**, no.6, 065205 (2015) doi:10.1103/PhysRevC.91.065205 [arXiv:1503.08666 [hep-ph]].
- [50] G. y. Shao, L. Chang, Y. x. Liu and X. l. Wang, *Phys. Rev. D* **73**, 076003 (2006) doi:10.1103/PhysRevD.73.076003 [arXiv:hep-ph/0602100 [hep-ph]].
- [51] M. B. Pinto, V. Koch and J. Randrup, *Phys. Rev. C* **86**, 025203 (2012) doi:10.1103/PhysRevC.86.025203 [arXiv:1207.5186 [hep-ph]].
- [52] J. W. Cahn and J. E. Hilliard, *J. Chem. Phys.* **28**, 258-267 (1958) doi:10.1063/1.1744102.
- [53] D. G. Ravenhall, C. J. Pethick and J. M. Lattimer, *Nucl. Phys. A.* **407**, 571-591 (1983) doi:10.1016/0375-9474(83)90667-X.
- [54] J. Randrup, *Phys. Rev. C* **79**, 054911 (2009) doi:10.1103/PhysRevC.79.054911 [arXiv:0903.4736 [nucl-th]].
- [55] D. N. Voskresensky, M. Yasuhira and T. Tatsumi, *Nucl. Phys. A* **723**, 291-339 (2003) doi:10.1016/S0375-9474(03)01313-7 [arXiv:nucl-th/0208067 [nucl-th]].